

Microstructural study of rare earth intermetallic single crystals by transmission electron microscopy

Y.J. Bi and J.S. Abell

School of Metallurgy and Materials, University of Birmingham, Birmingham B15 2TT (UK)

Abstract

Single crystals of RAI_2 and $RFe_{1.95}$ (R =rare earth) have been studied by transmission electron microscopy. It is found that $CeAl_2$ single crystal contains a few dendritic secondary phases and many $\{001\}$ growth faults. Analysis suggests that the growth faults could result from the coalescence of vacancies, which was possibly enhanced by the compositional deviation from stoichiometry. However, a $TbAl_2$ single crystal contains a number of large $\{111\}$ planar faults enriched in tungsten induced by crucible contamination. By substituting 1 at.% Tb with Ho, the existence of tungsten changed from planar to small spherical particles. Studies on a pseudo-single crystal of $(Tb_{0.27}Dy_{0.73})Fe_{1.95}$ show numerous $\{111\}$ stacking faults and many Widmanstätten precipitates. The influence of these crystal lattice imperfection and impurities on the magnetic behaviour is discussed.

1. Introduction

The achievement of large single crystals of rare earth compounds has increased the research in magnetism during the last decade [1]. However, many physical property measurements have been complicated by their dependence on sample quality, such as crystallinity, microstructural defects and impurity distribution *etc.* [2]. Therefore, more specific microstructural characterization on the available single crystals becomes necessary. Single crystals of the Laves phase compounds RAI_2 and RFe_2 (R =rare earth elements) have been extensively investigated for their magnetism and magnetostriction properties [3–6], although little work has been performed on characterization of the microstructural defects and their effects on physical properties [7–9].

In this work, a detailed microstructural characterization on as-grown single crystals of RAI_2 (R =Ce, Tb) and $(Tb_{0.27}Dy_{0.73})Fe_{1.95}$ has been carried out by transmission electron microscopy (TEM). The presence of impurities and crystal defects have been identified; and the possible influence of these imperfections on physical property measurements has been discussed.

2. Experimental details

Single crystals of RAI_2 (R =Ce, Tb or Tb (1% Ho)) were grown by the Czochralski method from a melt with nominal stoichiometric composition held in a tung-

sten crucible at the growth rate of 28 mm/h [10]. The as-grown crystal boules, initially assessed by Laue X-ray diffraction, are good quality single crystals. A pseudo-single crystal of $(Tb_{0.27}Dy_{0.73})Fe_{1.95}$ was prepared by the Czochralski technique with an induction-heated cold crucible. Examination by X-ray diffraction shows the presence of misorientations of about 5°. Specimens for TEM were cut from the as-grown crystal boules and prepared either by ion beam milling or standard twin jet electropolishing. Transmission electron microscopy was carried out either on a Philips EM400 with operating voltage of 100 kV or on a Joel 4000FX with accelerating voltage of 400 kV, the latter interfaced to a Link EDX analytical system.

3. Results and discussion

3.1. TEM observation and analysis of RAI_2

The microstructural examination of a $CeAl_2$ single crystal shows that it contains a few small non-faceted, dendrite-shaped secondary phases, many planar faults and single dislocations. Figure 1(a) shows a typical planar fault separated into regions with different contrast by dislocations. X-Ray energy dispersive (EDX) analysis of the secondary phases, which show no orientation relationships with the matrix, indicates that they have the composition varying between Ce_3Al_{11} and $CeAl_3$. Since $CeAl_3$ is formed by a peritectoid reaction between $CeAl_2$ and Ce_3Al_{11} [11], the dendritic phase might firstly be nucleated as Ce_3Al_{11} from the melt, and subsequently reacted with the surrounding matrix

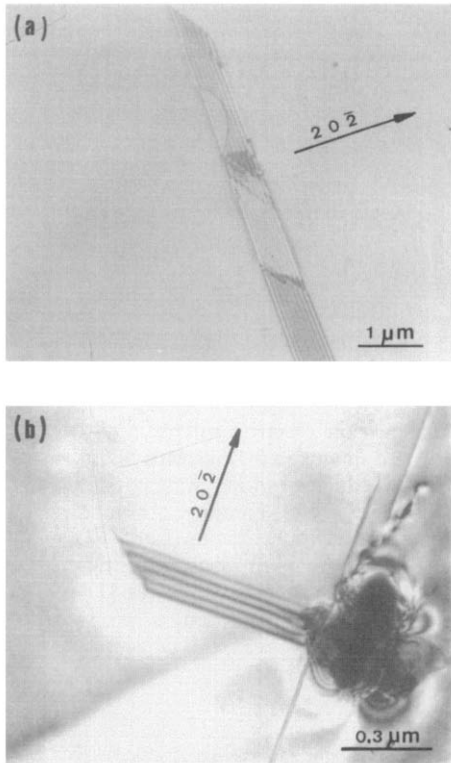


Fig. 1. (a) A typical $\{0 0 1\}$ plane stacking fault in CeAl₂ single crystals showing the regions with various contrast. (b) A dendritic secondary phase with the associated stacking faults.

during cooling to the peritectoid temperature. Since the peritectoid reaction is a solid state diffusion-controlled reaction, the process is limited to the surface of the Ce₃Al₁₁ phase. Both the planar faults and single dislocations are often associated with the dendritic phases (Fig. 1(b)). By focusing a small electron probe of 10 nm on an edge-on stacking fault, the EDX spectrum hardly shows any difference with the surrounding matrix, although a slight tendency of cerium enrichment in the fault is observed.

By both diffraction contrast study and standard trace analysis, the planar faults were determined to be $\{0 0 1\}$ plane stacking faults with intrinsic characteristics. Since the fringe contrast in a planar fault is due to the discontinuities of the planes intersecting the defect, the defect is, therefore, defined by a displacement vector \mathbf{R} . Further analysis facilitated with computer image simulation shows that the $\{0 0 1\}$ plane stacking faults have a displacement vector of $1/14\langle\bar{1} \bar{1} 4\rangle$, which is neither perpendicular to the habit plane nor in the plane. Since the stacking faults are of the intrinsic type, they could only arise by the coalescence of vacancies, *i.e.* they are growth faults. Lattice imaging by high resolution electron microscopy (HREM) confirms the result obtained by the diffraction contrast study (see Fig. 2).

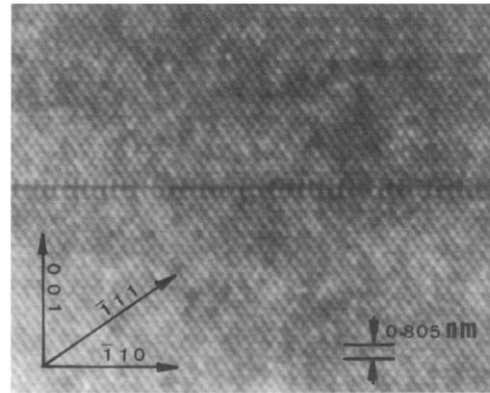


Fig. 2. A high resolution electron micrograph of an edge-on fault in CeAl₂ with beam direction down $\langle 1 1 0 \rangle$ showing the projected displacement along the $[0 0 1]$ and $[\bar{1} 1 0]$ directions.

The coalescence of vacancies on $\{0 0 1\}$ planes rather than on close-packed $\{1 1 1\}$ planes is not understood yet, although it may be related to the resultant low energy. On the other hand, a composition deviation from stoichiometry of CeAl₂ could result in the formation of the $\{0 0 1\}$ intrinsic faults [12]. For instance, any local deficiency of aluminium atoms would lead to the formation of vacancies which further coalesce during cooling to form Al-deficient stacking faults, as indicated by EDX analysis. The slow cooling rate during crystal growth would certainly allow the migration of excess vacancies to reach equilibrium. The observation of stacking faults associated with Al-rich phases suggests that during the solid state peritectoid reaction between Ce₃Al₁₁ and the surrounding matrix, the diffusion of aluminium atoms towards secondary phase interfaces resulted in a counter diffusion of vacancies to the matrix, thereby leading to the formation of $\{0 0 1\}$ plane stacking faults.

Studies on a CeAl₂ single crystal prepared from a slightly Al-deficient composition show that the crystal contains no secondary phases and only a few growth faults. This observation further suggests that the presence of planar faults may play a role in absorbing composition deviation from stoichiometry [13]. $\{0 0 1\}$ plane stacking faults have been reported in other compounds with either L1₂ structure [12] or A15 structure [14], where the faults resulted from the dissociation of $a_0\langle 0 0 1 \rangle\{0 0 1\}$ dislocations having displacement vectors perpendicular to their habit planes. However, recent work on an arc-melted Nb₃Al button [15] has shown the existence of $\{0 0 1\}$ plane growth faults.

A typical microstructure of as-grown TbAl₂ single crystals contains many planar defects with a "staircase" feature but no secondary phases, as shown in Fig. 3(a). Diffraction contrast analysis indicates that the defects have $\{1 1 1\}$ habit planes with no complete invisibility

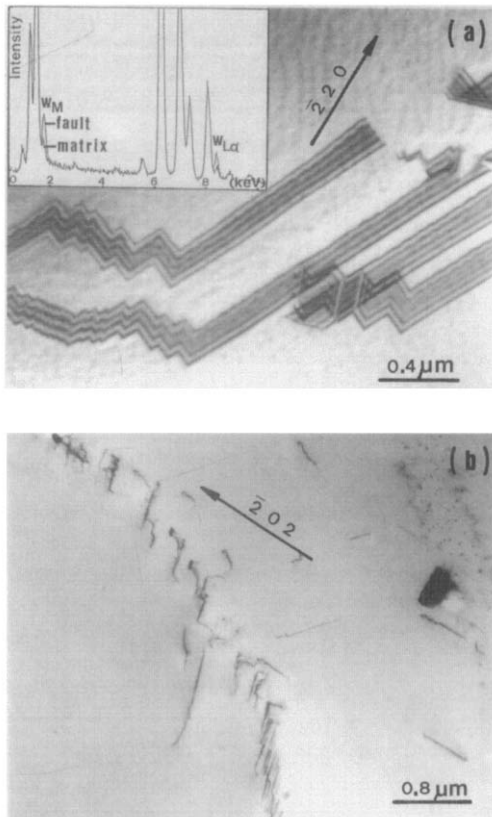


Fig. 3. (a) A few typical planar faults with the “staircase” feature in a TbAl_2 single crystal showing tungsten enrichment as shown in the inserted EDX spectrum. (b) When 1 at. % Tb was substituted by Ho, the large planar W-rich faults changed into smaller-sized faults and many W-rich precipitates.

conditions. EDX analysis with a small probe focused on edge-on faults shows that the planar faults have a tungsten-peak, although quantitative analysis is unfeasible (see the insert in Fig. 3(a)). The observation suggests that small tungsten atoms, which could only be present due to crucible contamination, might substitute for some of the aluminium atoms on $\{111\}$ planes to form large planar faults. Therefore, the planar faults would have a complex displacement vector, as indicated by the diffraction contrast study.

The observation of the W-rich planar defects suggests that when a small amount of tungsten impurity was introduced into the TbAl_2 crystal, the tungsten atoms preferentially substituted for aluminium on $\{111\}$ planes. When part of the Tb was substituted by 1 at. % Ho, the large planar faults were replaced by smaller-sized planar faults and associated spherical precipitates, sometimes around low angle grain boundaries (see Fig. 3(b)). Compositional analysis confirms that the precipitates with size smaller than 20 nm are W-rich phases with an undetectable amount of holmium.

The presence of tungsten impurity could strongly influence the magnetic properties of the single crystal

by influencing the domain wall motion. An earlier study on the domain structure of TbAl_2 single crystals by X-ray topography [4] has already shown some heavy domain wall pinning by unknown impurities. This observation may be interpreted as the effect of tungsten-rich planar faults. Although single dislocations and conventional stacking faults (formed by the removal or insertion of atomic layers) have been shown to have a very weak pinning effect on domain wall motion [9], the W-rich planar faults may act as thin secondary phase layers, which could strongly pin the magnetic domain walls. Although no magnetic domain structure measurement has been done on single crystals of TbAl_2 with 1 at. % Ho substitution, the existence of additional W-rich precipitates is expected to further degrade the magnetostrictive properties. The observation shows that the substitution of terbium with 1% of Ho resulted in the change of the distribution of W impurity in the TbAl_2 single crystals from large planar faults to smaller-sized faults and additional W-rich precipitates. The mechanism of this change is not yet understood.

3.2. TEM observation and analysis of $(\text{Tb}_{0.27}\text{Dy}_{0.73})\text{Fe}_{1.95}$

The $(\text{Tb}_{0.27}\text{Dy}_{0.73})\text{Fe}_{1.95}$ crystal contains many planar faults and a few plate-like Widmanstatten precipitates (WSP) as shown in Fig. 4. Image and diffraction pattern analysis indicates that the planar defects are stacking faults with $\{111\}$ habit planes, which is consistent with previous results on float zoned Terfenol-D crystals [8,16]. The Widmanstatten precipitates, which also have $\{111\}$ habit planes, and extend to a few micrometres and end on another precipitate, contain a large number of interfacial dislocations.

In the present study, no sign of twins has been observed in this crystal, which suggests that the crystal growth behaviour was different from the previously reported dendritic growth mechanism [17,18]. In the

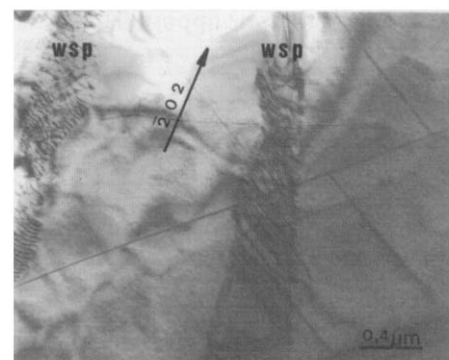


Fig. 4. A typical TEM micrograph of Czochralski-grown $(\text{Tb}_{0.27}\text{Dy}_{0.73})\text{Fe}_{1.95}$ showing many $\{111\}$ plane stacking faults and two plate-like Widmanstatten precipitates enclosed by interfacial dislocations.

case of the vertical float zoning or Bridgman growth at rates of 25 mm/h or higher [17,18], the solidification interface proceeded in a cellular or dendritic mode. However, during the present Czochralski growth at a slow rate (~ 15 mm/h), the growth front was believed to be planar rather than dendritic in nature [19].

Although the magnetostrictive properties of a Czochralski-grown rod shows improved behaviour due to the good crystallinity [19], the existence of the Widmanstätten precipitates is regarded as detrimental. Recent observation by Lorentz microscopy [9] indicated that the strain field around Widmanstätten precipitates could strongly deviate or sometimes pin the magnetic domain walls.

4. Conclusions

The formation of $\{001\}$ plane stacking faults in as-grown CeAl_2 single crystals is suggested to accommodate the deviation from stoichiometry of the compound. By carefully preparing the initial composition, the secondary phase and the Al-deficient stacking faults can be reduced.

Large $\{111\}$ planar faults in as-grown TbAl_2 single crystals were determined to be W-rich due to crucible contamination. By substituting Tb with 1% Ho, the large planar defects were replaced by smaller-sized planar faults and W-rich precipitates. Both W-rich planar faults and the precipitates will degrade the magnetic properties by pinning the domain wall motion.

Pseudo-single crystal of $\text{Tb}_{0.27}\text{Dy}_{0.73}\text{Fe}_{1.95}$ prepared by the Czochralski method contains numerous $\{111\}$ plane stacking faults and many Widmanstätten precipitates. The WSP has a detrimental effect on magnetic domain walls comparing with stacking faults.

Acknowledgments

The authors would like to thank Mr. A. Bradshaw and Mr. J. Sutton for their technical support. This work

is part of a SERC supported project on purification and single crystal preparation of reactive and refractory metals.

References

- 1 D. Gignoux and D. Schmitt, *J. Magn. Magn. Mater.*, **100** (1991) 99.
- 2 J.S. Abell, in K.A. Gschneidner, Jr. and L. Eyring (eds.), *Handbook on the Physics and Chemistry of Rare Earth*, Vol. 12, North-Holland, Amsterdam, 1989, p. 1.
- 3 E.D. Forgan, B.D. Rainford, S.L. Lee, J.S. Abell and Y.J. Bi, *J. Phys.-Condensed Matter*, **2** (1990) 10211.
- 4 G.D. Clark, B.K. Tanner and J.S. Abell, *J. Magn. Magn. Mater.*, **49** (1985) 317.
- 5 J.S. Abell and D.G. Lord, *J. Less-Common Met.*, **126** (1986) 107.
- 6 J.D. Verhoeven, J.S. Ostenson and E.D. Gibson, *J. Appl. Phys.*, **66** (1989) 772.
- 7 Y.J. Bi and J.S. Abell, *Scr. Metall. Mater.*, **29** (1993) 543.
- 8 Y.J. Bi, J.S. Abell and A.M.H. Hwang, *J. Magn. Magn. Mater.*, **99** (1991) 159.
- 9 M. Al-Jiboory, D.G. Lord, Y.J. Bi, J.S. Abell and A.M.H. Hwang, *J. Appl. Phys.*, **73** (1993) 6168.
- 10 Y.J. Bi, J.S. Abell and D. Fort, *Proc. Symp. 2nd Int. Conf. on Rare Earth Development and Application*, Beijing, China, IAP, 1991, p. 100.
- 11 K.H.J. Buschow and J.H.N. van Vucht, *Z. Metallkd.*, **57** (1966) 162.
- 12 W.O. Powers, J.A. Wert and C.D. Turner, *Philos. Mag. A*, **60** (1989) 227.
- 13 S.V. Sudareva, N.N. Buynov and Y.P. Romanov, *Phys. Met. Metall.*, **44** (1978) 114.
- 14 M. Aindow, J. Shyue, T.A. Gaspar and H.L. Fraser, *Philos. Mag. Lett.*, **64** (1991) 59.
- 15 L.S. Smith, T.T. Cheng and M. Aindow, *Proc. Symp. MRS Fall Meeting*, Boston, 1992, in press.
- 16 A.G. Jenner, D.G. Lord and C.A. Faunce, *IEEE Trans. Magn.*, **24** (1988) 1865.
- 17 A.E. Clark, J.D. Verhoeven, O.D. McMasters and E.D. Gibson, *IEEE Trans. Magn.*, **22** (1986) 973.
- 18 J.D. Verhoeven, E.D. Gibson O.D. McMasters and H.H. Baker, *Metall. Trans. A*, **18** (1987) 223.
- 19 Y.J. Bi, A.M.H. Hwang and J.S. Abell, *J. Magn. Magn. Mater.*, **104-107** (1992) 1471.